Plant Physiology and Biochemistry 145 (2019) 1–9

Contents lists available at ScienceDirect

Plant Physiology and Biochemistry

journal homepage: www.elsevier.com/locate/plaphy

Research article

Non-structural carbohydrate and hydraulic dynamics during drought and recovery in *Fraxinus ornus* and *Ostrya carpinifolia* saplings

Martina Tomasella[a], Valentino Casolo[b], Natalie Aichner[a], Francesco Petruzzellis[a], Tadeja Savi[c], Patrizia Trifilò[d], Andrea Nardini[a,*]

[a] *Dipartimento di Scienze della Vita, Università di Trieste. Via L. Giorgieri 10, 34127, Trieste, Italy*
[b] *Dipartimento di Scienze Agroalimentari, Ambientali e Animali, Università di Udine. Via delle Scienze 91, 33100, Udine, Italy*
[c] *Institute of Botany, Department of Integrative Biology and Biodiversity Research, BOKU, Gregor-Mendel-Straße 33, Vienna, 1190, Austria*
[d] *Dipartimento di Scienze Chimiche, Biologiche, Farmaceutiche ed Ambientali, Università di Messina, Viale Ferdinando Stagno d'Alcontres 31, 98166, Messina, Italy*

ARTICLE INFO

Keywords:
Hydraulic failure
NSC
Recovery
Starch
Water use strategies

ABSTRACT

The maintenance of hydraulic function during and after a drought event is crucial for tree survival, but the importance of non-structural carbohydrates (NSCs) in the recovery phase is still debated. We tested whether higher NSC availability facilitates post-drought hydraulic recovery, by applying a short-term drought (S_{dr}) and a long-term drought combined with shading (L_{dr+sh}) in *Fraxinus ornus* and *Ostrya carpinifolia*. Plants were then re-irrigated and recovery was checked 24 h later, by measuring water potential, stem percentage loss of hydraulic conductance (PLC) and NSC content. The relative magnitude of hydraulic and carbon constraints was also assessed in desiccated plants. During drought, PLC increased only in *F. ornus,* while it was maintained almost constant in *O. carpinifolia* due to tighter stomatal control of xylem pressure (i.e. more isohydric). In *F. ornus*, only S_{dr} plants maintained high NSC contents at the end of drought and, when re-irrigated, recovered PLC to control values. Whereas hydraulic failure was ubiquitous, only *F. ornus* depleted NSC reserves at mortality. Our results suggest that preserving higher NSC content at the end of a drought can be important for the hydraulic resilience of trees.

1. Introduction

The widespread episodes of tree die-back and mortality observed over the last decades under extreme drought and heat waves have been hypothesized to be caused by two main physiological processes: hydraulic failure and carbon starvation (McDowell et al., 2008). The first refers to the irreversible impairment of plant water transport, which induces tree desiccation and is generally quantified in terms of percentage loss of xylem hydraulic conductance (PLC; McDowell et al., 2008, 2011). The second is related to the massive loss of carbohydrates required for sustaining minimum primary and secondary metabolic functions (McDowell et al., 2011), and is often quantified in terms of non-structural carbohydrate (NSC) content (Hartmann et al., 2013; Hoch et al., 2003; Nardini et al., 2016). NSCs include starch, which is the main storage compound in woody plants, and soluble sugars which derive directly from photosynthesis or from starch depletion, and are involved in multiple physiological functions such as respiration, turgor maintenance, phloem transport, hydraulic repair, signalling and defence (Hartmann and Trumbore, 2016). A global synthesis conducted on healthy plants from different functional types and biomes showed that starch, according to its storage function, typically undergoes seasonal fluctuations, and transitory starch depletion is common. On the other hand, soluble sugar content is generally maintained above certain thresholds and rarely decreases to very low values (Martinez-Vilalta et al., 2016).

Under drought, xylem embolism formation derives from a purely physical process involving gas entry into xylem conduits owing to increasing xylem tension (Nardini et al., 2017; Tyree and Zimmermann, 2002), while NSC depletion mainly depends on the imbalance between carbon uptake via photosynthesis and carbon substrate demand (Mooney, 1972). This imbalance can also be restricted to some organs (Hartmann et al., 2013; Kannenberg et al., 2017; Klein et al., 2014). On the premise that the two processes could be interdependent (McDowell et al., 2011; Sevanto et al., 2014), it has been hypothesized that the occurrence of either hydraulic failure or carbon starvation may be related to a species' water use strategy (McDowell et al., 2008). Following the framework adopted by Tardieu and Simmoneau (1998), plants facing drought fall in a continuum between tight (isohydric) and weak

---

[*] Corresponding author.
E-mail address: nardini@units.it (A. Nardini).

https://doi.org/10.1016/j.plaphy.2019.10.024
Received 8 August 2019; Received in revised form 14 October 2019; Accepted 17 October 2019

(anisohydric) stomatal regulation of leaf water potential (Klein, 2014). Different interpretations and related metrics have been recently proposed to quantify the an/isohydric behaviour (Martínez-Vilalta et al., 2014; Meinzer et al., 2016), leading to different species rankings (Li et al., 2019; Martínez Vilalta and Garcia-Forner, 2017; Meinzer et al., 2016). Moreover, species-specific plasticity of an/isohydry dependent on the growth environment, has also been suggested (Fu and Meinzer, 2019; Hochberg et al., 2018). Relatively isohydric species were hypothesised to be more prone to carbon starvation compared to more anisohydric ones, because of earlier and/or prolonged stomatal closure aimed at reducing water loss and consequent dramatic drops in plant water potential (McDowell et al., 2008). However, it has also been pointed out that the an/isohydry of a species may not necessarily be caused by its stomatal regulation and, consequently, this classification would not help to identify specific mechanisms of tree mortality under drought (Martínez Vilalta and Garcia-Forner, 2017). Moreover, length and intensity of drought (Mitchell et al., 2013), modulation of growth rates under stress (Deslauriers et al., 2014), tree size and age (Trugman et al., 2018), competition (Caldeira et al., 2015) and accessibility to deep water sources (Nardini et al., 2016) all contribute to the total plant carbon balance.

Albeit only very low NSC contents may induce death of plants in absence of drought stress (Wiley et al., 2017), previous studies showed that NSCs are involved in mechanisms preventing drought-induced hydraulic failure and promote plant survival under water shortage (Bloemen et al., 2016; O'Brien et al., 2014; Sevanto et al., 2014). Moreover, survival and competitive success of tree species in regions affected by an increased frequency of drought events may depend on their resilience capability. Recovery processes such as production of new organs, growth of new functional xylem (Brodribb et al., 2010; Tomasella et al., 2019; Trugman et al., 2018) and refilling of embolized conduits (Klein et al., 2018) may require the use of substantial NSC reserves, especially if photosynthesis and/or phloem transport are still impaired in the short term after drought relief (Sevanto, 2014).

The refilling of gas-filled conduits can be ascribed to several processes: root/stem positive pressure when soil is fully saturated and transpiration is low (Hao et al., 2013), water uptake through leaf and bark surfaces (Mayr et al., 2014), and osmotically-driven xylem parenchyma-mediated refilling under moderate tension, commonly described as novel refilling (e.g. Brodersen and McElrone, 2013; Nardini et al., 2011; Ogasa et al., 2010). Novel refilling is a process that supposedly requires accumulation of soluble NSCs in order to locally reduce the osmotic potential in the xylem conduits, thus promoting water inflow from the surrounding living cells to the refilling conduits (Nardini et al., 2011; Secchi and Zwienieki, 2016; Trifilò et al., 2019).

Starch availability in stems could apparently play a fundamental role in the hydraulic repair, either via new xylem build-up, or based on active osmotic process, as starch depletion and subsequent increase in sucrose concentration have been observed in living parenchyma cells next to xylem conduits at the onset of refilling (Salleo et al., 2004, 2009). In accordance, Savi et al. (2016) found that stem soluble NSC content at the end of drought was correlated with the hydraulic recovery capacity across four different woody angiosperms. Therefore, together with preserved parenchyma cells functionality and membrane integrity (Secchi et al., 2017), the success of this process should depend on the availability of sufficient NSCs (Trifilò et al., 2019). Consequently, hydraulic recovery could be favoured in plants with high stem NSC content and, vice versa, a lower recovery capability should characterize plants with depleted NSC pools due to prolonged drought and/or an isohydric strategy (Trifilò et al., 2017).

In the present study, we analysed water relations and stem hydraulics of *Fraxinus ornus* and *Ostrya carpinifolia* under drought and following re-irrigation. These two species, often sharing the same habitat, have been threatened by recent anomalous summer droughts (Nardini et al., 2003, 2013, 2014). Our main goal was to investigate whether the short-term (24 h) hydraulic recovery capacity of these species after drought relief could be related to the availability of stem NSCs at the end of drought, which might be influenced by the species' water use strategies. Our experimental approach consisted in comparing a short term drought treatment, which should not alter total NSC contents, to a long-term drought coupled to partial shading, which is expected to promote stem NSC consumption (Sevanto et al., 2014; Wiley et al., 2017). We therefore tested the hypothesis that, whenever a relatively weak stomatal regulation of water potential (supposedly related to a more anisohydric behaviour) induces a significant increase in stem PLC, a higher NSC availability at the end of drought would favour the post-drought hydraulic recovery. Given the recent results showing a non-ubiquitous occurrence of carbon starvation at mortality (Adams et al., 2017), we additionally analysed stem PLC and NSC content at the onset of complete leaf desiccation.

2. Materials and methods

2.1. Experimental design and plant material

On April 2017, two-year old saplings of *Fraxinus ornus* L. and *Ostrya carpinifolia* Scop. (50 plants per species; height of 50–60 cm and 60–70 cm, respectively) were provided by a public nursery (Vivai Pascul, Regional Forestry Service, Tarcento, Italy), and were transplanted in 3.5 l pots and randomly allocated in a greenhouse of the botanical garden of the University of Trieste (Italy). The substrate was a 1:1 mix (v/v) of a lightweight substrate (Savi et al., 2013) and a commercial potting compost (BRIL substrate, Geotec Srl, Bolzano, Italy). A slow release fertilizer (COMPO Agro Specialities Srl, Monza, Italy) was added to each pot in April (8 g) and May (5 g). Pots were irrigated at field capacity every 1–3 days, until the start of experimental treatments. Twenty-five plants per species were maintained under greenhouse light conditions for the whole experiment and were divided in two groups: one was irrigated daily to field capacity for the whole experiment (*Ctrl*, control treatment, n = 6–7), the other was subjected to an abrupt drought stress by suspending irrigation from July 4th for 10–17 days, depending on individual water consumption rate (S_{dr}, short-term drought treatment). From May 25th, 2017, the other 25 plants per species were placed under a shading net filtering 75% of Photosynthetic Photon Flux Density (PPFD), and were subjected to mild drought stress from May 29th. Initially, drought in these plants was imposed to induce substantial and fast stomatal closure, i.e. to decrease leaf conductance to water vapour (g_L) by about 10–50% with respect to *Ctrl* plants. Afterwards, plants were maintained at those stress levels for ~30 days, regulating the daily amount of irrigation on the basis of plant daily water loss, which was assessed by weighing the pots on a 24 h interval before the beginning of the stress treatment. Given that plants differed in their water consumption and in the time needed to reach the target g_L, the total duration of the drought period for these plants (L_{dr+sh}, long-term drought + shade treatment) was 30–53 days. At the end of the drought stress period, six S_{dr} and six L_{dr+sh} plants were re-irrigated at field capacity (S_{dr}-*R*, short-term drought treatment followed by recovery, and L_{dr+sh}-*R*, long-term drought + shade treatment followed by recovery, respectively; L_{dr+sh}-*R* plants were maintained in the shade) and measured 24 h later to assess the eventual recovery of physiological parameters. At the end of the study, six to seven L_{dr+sh} plants per species were left in the shade and without irrigation until complete leaf desiccation, (*Des*, desiccation treatment), which occurred between 2nd and 4th August, and were all measured on August 4th. A scheme of the experimental design is provided in Fig. 1.

2.2. Micro-climatic data

On May 26th, 2017, two USB data logger sensors (EL-USB-2, Lascar Electronics Inc., Salisbury, UK) recording air temperature and relative humidity (RH) on an hourly basis were placed in the greenhouse in proximity of the study plants. Sensors were placed at a height of

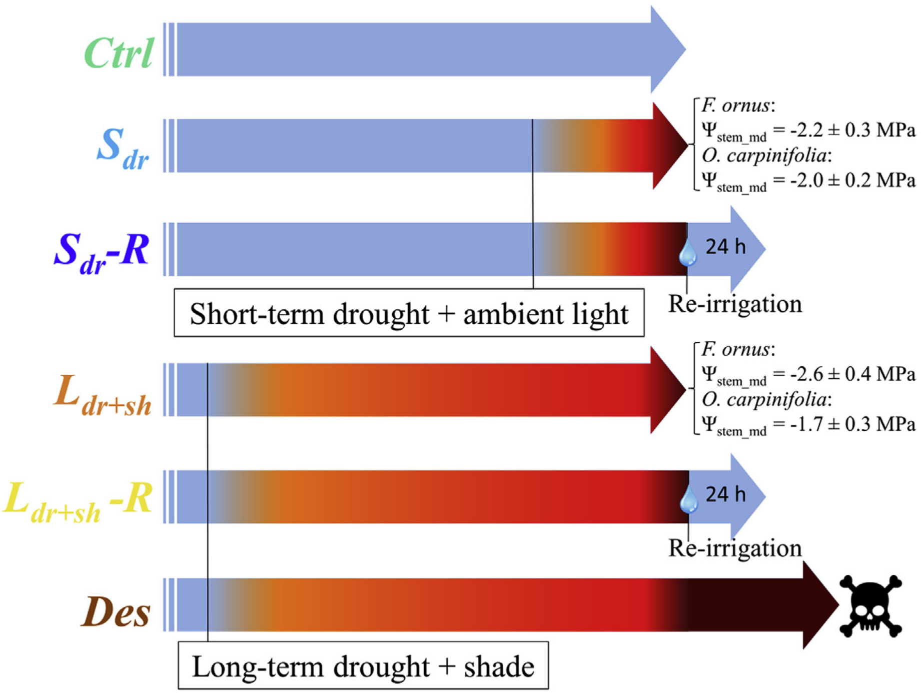

Fig. 1. Scheme of the experiment. *Ctrl* plants were always maintained well irrigated, S_{dr} and S_{dr}-*R* plants were subjected to a short period of drought; L_{dr+sh}, L_{dr+sh}-*R* and *Des* plants were subjected to prolonged drought coupled to shading. S_{dr} and L_{dr+sh} plants were harvested and measured at the end of the drought period, S_{dr}-*R* and L_{dr+sh}-*R* plants one day after re-irrigation, *Des* plants at complete leaf desiccation. n = 6–7 in each treatment.

180 cm, one inside the shading net and one outside. PPFD (μmol s^{-1} m^{-2}) was periodically measured with a quantum sensor (model HD 9021, Delta OHM srl, Padova, Italy) at the top of plants (130 cm). During the experiment, daily temperature outside and inside the shading net was 25.7 ± 0.3 and 25.5 ± 0.2 °C (values are mean ± SE), and maximum temperatures reached 43 °C and 40 °C, respectively. Mean daily RH registered by both data loggers was 62 ± 1% (see Supplementary Fig. S1). Maximum PPFD reached values of 200 μmol s^{-1} m^{-2} and 920 μmol s^{-1} m^{-2} inside and outside the shading net, respectively.

2.3. Leaf water relations

Leaf conductance to water vapour (g_L, mmol m^{-2} s^{-1}) was assessed with a steady-state porometer (SC-1, Decagon Devices Inc., Pullman, USA) between 11.00 h and 14.00 h (solar time) on mature leaves. Measurements of g_L were performed: a) every 1–3 days in L_{dr+sh} plants (see Supplementary Fig. S2), to modulate the irrigation volumes; b) at the end of the drought period in all plants; c) before harvest (i.e. 24 h after rehydration) in L_{dr+sh}-*R* and S_{dr}-*R* plants, to assess the recovery of stomatal aperture.

Leaf water potential was measured on mature leaves using a pressure chamber (mod. 1505D, PMS Instrument co., Albany, OR, USA). Midday leaf (Ψ_{leaf_md}, MPa) and stem xylem water potential (Ψ_{stem_md}, MPa) were measured between 11.00 h and 14.00 h (solar time) on one leaf per plant, right before hydraulic measurements (see below). Ψ_{stem_md} was assessed in leaves that were bagged in cling film and covered with aluminium foil in the early morning. Leaf water potential was measured in the two recovery groups (L_{dr+sh}-*R* and S_{dr}-*R*) also the day after re-irrigation, before 08.00 h (early morning leaf water potential, Ψ_{leaf_em}, MPa). Additionally, Ψ_{leaf_md} was periodically monitored on L_{dr+sh} plants during the dry-down period in order to regulate the daily amounts of irrigation water (see above).

Osmotic potential at full turgor (π_0) and water potential at turgor loss point (Ψ_{tlp}, MPa) were measured in leaves that were wrapped in cling film and detached from the plant prior PLC measurements. The procedure for π_0 and Ψ_{tlp} calculation followed Bartlett et al. (2012) with some modifications according to Petruzzellis et al. (2019). Two leaves per individual were fully rehydrated by immersing their petiole in distilled water for 24 h: one leaf was used to measure leaf dry matter content (LDMC, mg g^{-1}), and the other was immersed for 2 min in liquid nitrogen while bagged in cling film and ground to fine pieces. The first leaf was used to measure the fresh weight after full hydration (FW) and the dry weight after oven drying for 24 h at 70 °C (DW). LDMC was calculated as:

$$\mathrm{LDMC} = \mathrm{DW}\ \mathrm{FW}^{-1}$$

Ground leaves wrapped in cling film were stored in small airtight plastic containers at −20 °C until analysis. The water potential of the ground leaf material, that corresponds to its incorrect osmotic potential at full turgor ($\pi_{0,incorr}$), was measured with a dewpoint hygrometer (WP4, Decagon Devices Inc., Pullman, USA) after leaving the plastic containers at laboratory temperature for 10 min. The corrected osmotic potential at full turgor (π_0) was calculated from $\pi_{0,incorr}$ taking into account differences in LDMC as follows:

$$\pi_0 = (0.5303 \times \pi_{0,incorr}) - (0.0019 \times \mathrm{LDMC})$$

Ψ_{tlp} was then calculated as:

$$\Psi_{tlp} = 1.31 \times \pi_0 - \qquad 0.03$$

2.4. Percentage loss of xylem hydraulic conductance

Percentage loss of xylem hydraulic conductance (PLC, %) was assessed in the main stem at the end of the drought period in *Ctrl*, L_{dr+sh}, S_{dr} and *Des* plants, and after recovery in L_{dr+sh}-*R* and S_{dr}-*R* plants (n = 6–7). PLC measurements in *Ctrl* plants were distributed along the measurement period of the other plant groups. The main stem was cut under water 4 cm above the root collar and several consecutive cuts (1 cm each) were immediately made under clean water at the two ends of the shoot in order to relax xylem tension and avoid spurious gas entry in the xylem conduits (Trifilò et al., 2014). A 20 cm long segment without ramifications was finally obtained and thin cuts were made under water with a razor blade at both cut ends, right before connecting one end to a custom-made hydraulic apparatus. The perfusion solution was degassed, filtered (0.2 μm) mineral water with 10 mM KCl added (see Nardini et al., 2007). Native stem hydraulic conductance (k_i) was measured gravimetrically under low water pressure (4 kPa, generated

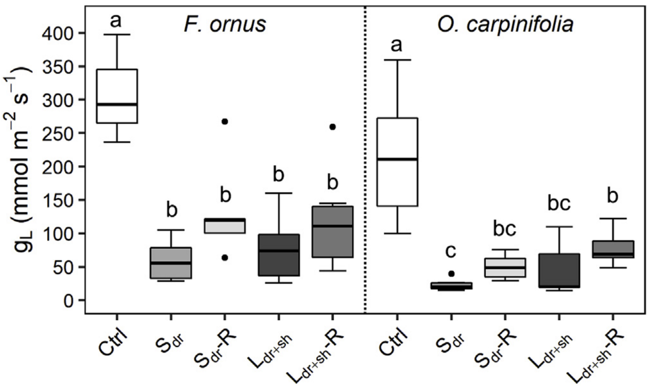

Fig. 2. Leaf conductance to water vapour (g_L) measured in *F. ornus* and *O. carpinifolia* at the end of drought period (in *Ctrl*, S_{dr} and L_{dr+sh}) and at recovery (in S_{dr}-*R* and L_{dr+sh}-*R*). Different letters indicate significant differences among groups, within the same species ($P < 0.05$). *Ctrl* = control well-irrigated; S_{dr} = short-term drought; S_{dr}-*R* = short-term drought followed by recovery; L_{dr+sh} = long-term drought + shade; L_{dr+sh}-*R* = long-term drought + shade followed by recovery.

by a water reservoir placed 40 cm above the sample) by collecting the solution at the extremity of the stem segment at 30–60 s intervals in 1.5 ml Eppendorf tubes filled with a piece of sponge. The sample was then flushed for 5 min at high pressure (0.15 MPa), generated in a captive air water tank connected to the apparatus. Flush duration was previously checked to be sufficient to remove all emboli and therefore to reach the maximum stem hydraulic conductance (k_{max}), which was measured as described above for k_i. PLC was calculated as:

$$PLC = 100 \times [1- (k_i\, k_{max}{}^{-1})]$$

2.5. Stem non-structural carbohydrate content

For NSC analysis, a 5 cm long stem segment was cut next to the one used for hydraulic measurements. Bark and wood were separated, microwaved for 3 min at 700 W in order to stop enzymatic activity, oven-dried at 70 °C for 24 h and stored at −20 °C until sugar extraction. After being ground to fine powder, 20 mg of sample were suspended in 300 µl of 80% ethanol and transferred in water bath at 80 °C for 30 min. After centrifugation at 14,000 rpm, the supernatant was transferred in a 1.5 ml Eppendorf tube, the pellet was re-suspended and sugars extracted again as above. The collected supernatant from the two extractions was pooled together and dried at 55 °C until complete evaporation of the solvent. The pellet resulted from evaporation was suspended in 500 µl of 50 mM Tris-HCl (pH 7.5) and incubated at 80 °C for 30 min. The resulting supernatant was centrifuged, added to the oven-dried sugars remained from ethanol evaporation and stored at −20 °C for soluble sugars analysis. For starch analysis, the remaining pellet from sugar extraction was suspended in 1 mL of 0.4 M sodium acetate buffer solution, boiled for 1 h at 100 °C and cooled to room temperature. 100 U α-Amylase (from *Aspergillus orizae*, Sigma-Aldrich, Louis, MO, USA) and 25 U Amyloglucosidase (from *Aspergillus nigrae*, Sigma-Aldrich, Louis, MO, USA) were added to each sample in order to break down starch to glucose. Samples were incubated overnight in a 55 °C water bath, boiled for 3 min and centrifuged at 12,000 rpm for 5 min. Soluble sugars and starch content was estimated through the Anthrone method (Yemm and Willis, 1954). Anthrone was dissolved in sulphuric acid in a 1 g l^{-1} solution and kept in the dark. 5–25 µl of sample were placed in microplates and the Anthrone reagent was added to reach 200 µl solution and mixed. Before absorbance reading at 620 nm in a multilabel plate reader (Victor 3, PerkinElmer Inc., Waltham, USA), the microplates were placed on ice for 10 min, in the oven at 100 °C for 20 min and cooled down at room temperature for 20 min. Calibration curves converting absorbance to glucose concentration were obtained through the use of standard solutions of glucose and amylose, respectively used for soluble sugars and starch content estimation. Amylose followed the same treatment of the pellet of samples used for starch analysis.

2.6. Statistics

All statistical analyses were performed with R software (R Core Team, 2017). The effect of the different treatments was tested separately for each parameter and for each species independently. When normality of residuals and homogeneity of variances assumptions were not violated, one-way ANOVA analysis through 'aov' function in 'stats' R package was used, setting the selected parameter as the response variable and treatment as the explanatory variable. For significant tests (α = 0.05), Tukey's Honestly Significant Differences post hoc analysis was carried out through 'TukeyHSD' function in 'stats' R package. Generalized least squares (GLS) analysis was performed when homogeneity of variances assumption was violated, using 'gls' function with the 'varIdent' variance structure from the 'nlme' R package (Pinheiro et al., 2016). This analysis was followed by Tukey's Honestly Significant Differences post hoc analysis and p-values were adjusted using Bonferroni-Holm method. Values in figures are given as median, 25th and 75th percentile.

3. Results

3.1. Leaf water relations

Both L_{dr+sh} and S_{dr} drought treatments significantly impacted water relations of the study species. In particular, with respect to *Ctrl* plants, 80% lower g_L was recorded in L_{dr+sh} and S_{dr} plants in both species at the end of the imposed drought (Fig. 2), and Ψ_{leaf_md} dropped on average from ∼ −1.0 MPa to −2.5 MPa and −2.0 MPa, in *F. ornus* and *O. carpinifolia*, respectively, with no difference between L_{dr+sh} and S_{dr} treatments (Fig. 3a). At the end of the drought period, Ψ_{stem_md} was similar to Ψ_{leaf_md} in both species and treatments. The L_{dr+sh} treatment induced a reduction in the osmotic potential at full turgor (π_0) by about 0.7 MPa in *F. ornus* and 0.5 MPa in *O. carpinifolia*, and this resulted in a decline of Ψ_{tlp}, which reached −2.6 and −2.1 MPa, respectively. On the other hand, the S_{dr} treatment did not induce any significant osmotic adjustment in both species (Table 1). Following re-irrigation, the recovery in g_L was not significant in both drought treatments and species (Fig. 2). Ψ_{leaf_md} and Ψ_{stem_md} of *F. ornus* saplings increased by ∼1 MPa in L_{dr+sh}-*R* plants, and became even less negative in S_{dr}-*R* plants than in *Ctrl* plants. *O. carpinifolia* recovered water potentials to *Ctrl* values only in S_{dr}-*R* plants, whereas a smaller and non-significant increase in Ψ_{leaf_md} and Ψ_{stem_md} was observed in L_{dr+sh}-*R* plants (Fig. 3a and b). In both species, Ψ_{leaf_em} was similarly close to −0.9 MPa in L_{dr+sh}-*R* and S_{dr}-*R* plants (Fig. 3c). For both species and stress treatments, re-irrigation did not induce significant changes in π_0 and Ψ_{tlp} with respect to the end-stress values (Table 1).

3.2. Percentage loss of xylem hydraulic conductance

During the experiment, embolism levels and dynamics were overall different between the two species (Fig. 4). In *F. ornus*, *Ctrl* plants had PLC averaging 50%, and at the end of the stress treatments L_{dr+sh} and S_{dr} plants reached PLC of 78 ± 5% and 76 ± 2%, respectively (mean ± SE). After drought relief, PLC of *F. ornus* did recover to *Ctrl* values in the S_{dr}-*R* group, but not in L_{dr+sh}-*R* plants. In *O. carpinifolia* average PLC of *Ctrl* plants was 18% and did neither significantly increase when plants were subjected to the drought treatments, nor significantly change after re-irrigation. In both species, no difference in PLC between L_{dr+sh} and S_{dr} plants was observed. Plants which were brought to complete desiccation (*Des*) reached PLC values between 90

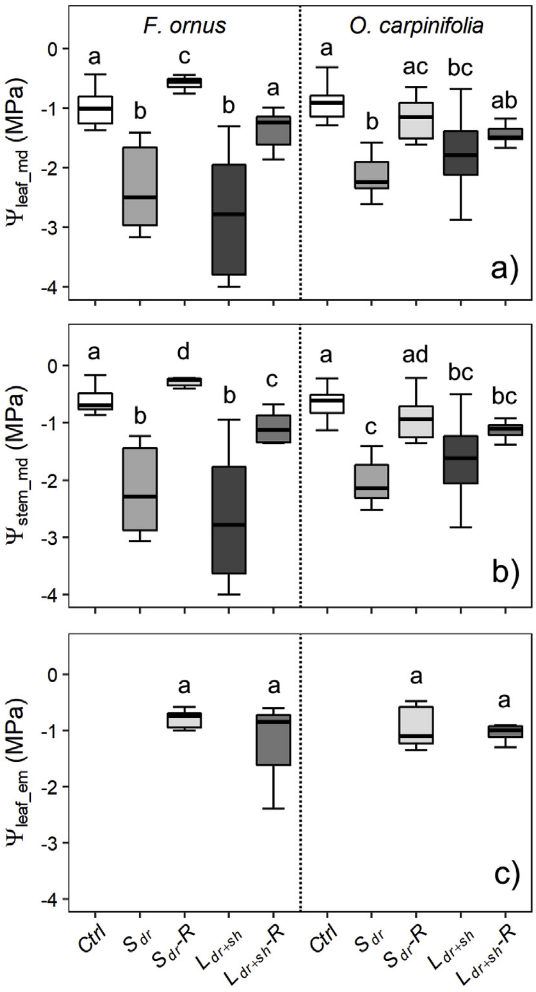

Fig. 3. Midday leaf (Ψ_{leaf_md}, a), midday stem (Ψ_{stem_md}, b) and early morning leaf (Ψ_{leaf_em}, c) water potentials of *F. ornus* and *O. carpinifolia* at the end of the experiment. Ψ_{leaf_em} was measured only in re-irrigated groups (*S_{dr}-R* and *L_{dr+sh}-R*). Different letters indicate significant differences among groups, within the same species ($P < 0.05$). *Ctrl* = control well-irrigated; *S_{dr}* = short-term drought; *S_{dr}-R* = short-term drought followed by recovery; *L_{dr+sh}* = long-term drought + shade; *L_{dr+sh}-R* = long-term drought + shade followed by recovery.

and 100% in both species.

3.3. Stem non-structural carbohydrate content

Ctrl plants of *F. ornus* had higher soluble NSC and starch content than *O. carpinifolia*, resulting in double and triple total NSC content in wood and bark, respectively (Fig. 5). NSC dynamics resulting from stress and recovery treatments were also different between the two study species. In particular, in *L_{dr+sh}* plants of *F. ornus* (i.e. subjected to prolonged drought accompanied by shading), total NSC reserves decreased by ~50% in both wood and bark tissues with respect to *Ctrl* plants, and this was mainly driven by starch depletion (Fig. 5). Starch and soluble NSC content did not significantly change after re-irrigation (*L_{dr+sh}-R* plants). In the case of *O. carpinifolia*, NSC content of *L_{dr+sh}* plants tended to increase with respect to *Ctrl* plants, and soluble as well as total NSC content in the wood were significantly higher in *L_{dr+sh}-R* than in *Ctrl*. In *F. ornus*, *S_{dr}* plants had similar bark NSC than *L_{dr+sh}*, but relatively high NSC contents in their wood. In particular, starch content was ~50% (corresponding to 18 mg g^{-1}) higher in *S_{dr}* than in *L_{dr+sh}* plants (non-significant) and similar to that of *Ctrl* ones. In *O. carpinifolia,* NSC content was similar in *S_{dr}* and *Ctrl*, but re-irrigation did not induce significant variations in NSC concentration.

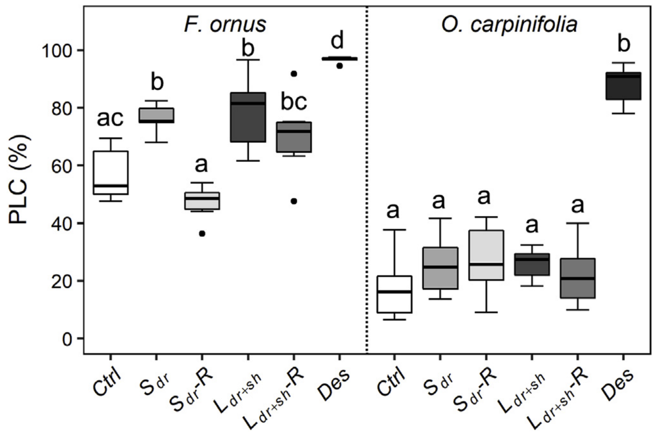

Fig. 4. Percentage loss of xylem hydraulic conductance (PLC) measured in stems of *F. ornus* and *O. carpinifolia* at the end of the experiment. Different letters indicate significant differences among groups, within the same species ($P < 0.05$). *Ctrl* = control well-irrigated; *S_{dr}* = short-term drought; *S_{dr}-R* = short-term drought followed by recovery; *L_{dr+sh}* = long-term drought + shade; *L_{dr+sh}-R* = long-term drought + shade followed by recovery, *Des* = leaf desiccation.

In *F. ornus*, large variability was observed in wood NSC concentration of *Ctrl* and especially *S_{dr}* plants. Of the almost 45 mg g^{-1} total NSC concentration range of values observed between the 25th and the 75th percentile, starch was responsible for about 35 mg g^{-1} variation (Fig. 5c).

In *F. ornus* saplings brought to death (*d* group), stem NSCs were further depleted with respect to *Ctrl* plants in both wood and bark tissues. In *O. carpinifolia*, instead, a further 30 mg g^{-1} increase in bark soluble sugars was detected, although total NSC content did not significantly change in both wood and bark tissues (Fig. 5).

4. Discussion

In the present study we found interesting differences between *F. ornus* and *O. carpinifolia* saplings in terms of hydraulic strategies and

Table 1

Osmotic potential at full turgor (π_0) and water potential at turgor loss point (Ψ_{tlp}) measured in *F. ornus* and *O. carpinifolia* in the different treatments. Values are means ± SEM. Different letters indicate significant differences among treatments within the same species ($P < 0.05$). *Ctrl* = control well-irrigated; *S_{dr}* = short-term drought; *S_{dr}-R* = short-term drought followed by recovery; *L_{dr+sh}* = long-term drought + shade; *L_{dr+sh}-R* = long-term drought + shade followed by recovery.

Treatment	F. ornus		O. carpinifolia	
	π_0 (MPa)	Ψ_{tlp} (MPa)	π_0 (MPa)	Ψ_{tlp} (MPa)
Ctrl	−1.28 ± 0.06^{a}	−1.71 ± 0.08^{a}	−1.14 ± 0.16^{a}	−1.53 ± 0.21^{a}
S_{dr}	−1.38 ± 0.05^{a}	−1.84 ± 0.07^{a}	−1.48 ± 0.05 ^{ab}	−1.98 ± 0.07 ^{ab}
S_{dr}-R	−1.42 ± 0.08^{a}	−1.90 ± 0.11^{a}	−1.35 ± 0.08 ^{ab}	−1.80 ± 0.10 ^{ab}
L_{dr+sh}	−1.93 ± 0.08^{b}	−2.56 ± 0.08^{b}	−1.61 ± 0.13^{b}	−2.15 ± 0.17^{b}
L_{dr+sh}-R	−1.69 ± 0.07 ^{ab}	−2.24 ± 0.08 ^{ab}	−1.70 ± 0.05^{b}	−2.27 ± 0.06^{b}

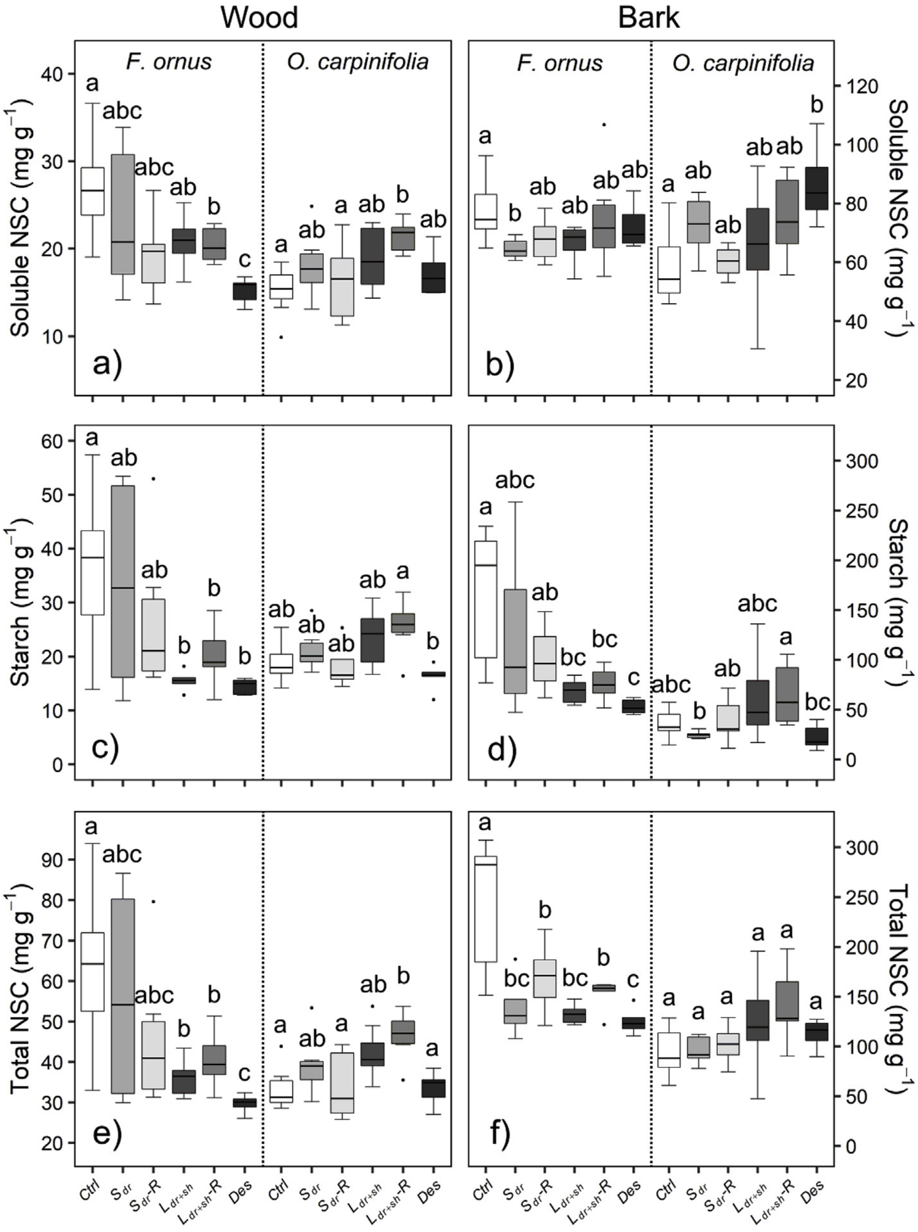

Fig. 5. Soluble NSC (a, b), starch (c, d) and total NSC (e, f) measured in wood and bark of *F. ornus* and *O. carpinifolia* stems. Please note that different scales are used for NSC content in the different panels. Different letters indicate significant differences among groups, within the same species ($P < 0.05$). *Ctrl* = control well-irrigated; S_{dr} = short-term drought; S_{dr}-*R* = short-term drought followed by recovery; L_{dr+sh} = long-term drought + shade; L_{dr+sh}-*R* = long-term drought + shade followed by recovery, *Des* = leaf desiccation.

NSC content under drought stress and subsequent recovery. The principal aim of this study was to test whether a different stem NSC availability at the end of a drought period has any impact on the possible hydraulic recovery after drought relief. This was actually the case for *F. ornus,* in that the high PLC registered at the peak of drought did recover to control (*Ctrl*) values only in S_{dr} plants, which maintained high wood NSC contents. In L_{dr+sh} ones, prolonged stomatal closure coupled to shading induced the depletion of NSC reserves. On the other hand, in *O. carpinifolia* both drought treatments did not induce embolism formation (PLC was similar to *Ctrl* plants) or NSC depletion, due to a tighter stomatal control of xylem pressure drop.

4.1. Water use strategies and NSC dynamics under drought

Under well watered conditions, *F. ornus* plants already had ~50% PLC in the stem albeit experiencing the same Ψ_{stem_md} as *O. carpinifolia* plants, which instead had low native embolism levels (~20% PLC; Fig. 4). Considering that plants were maintained outdoor in the nursery, the high PLC in *F. ornus* might arise from residual winter embolism in the older xylem conduits. This was possibly flushed or dissolved in *O. carpinifolia* by generation of root or stem pressure (Young et al., 2018), as revealed by typical bleeding of xylem sap from cut stems of this species in springtime just before bud break (personal observation).

Albeit the drought treatments were applied using the same criteria in both species and similar reductions in g_L with respect to *Ctrl* plants were induced, average values of g_L were ~50% lower in *O. carpinifolia* than in *F.ornus,* in both L_{dr+sh} and S_{dr} plants (Fig. 2). This resulted in a smaller drop of Ψ_{stem_md} at the end of the drought in *O. carpinifolia*. Stomatal control of xylem pressure apparently allowed *O. carpinifolia* to prevent embolism formation, as no significant increase in PLC was recorded with respect to *Ctrl* plants, while in *F. ornus* the marked drop of Ψ_{stem_md} caused further embolism build-up. A more isohydric behaviour intended as embolism avoidance, i.e. early stomatal closure aimed at preventing embolism formation, can be evaluated comparing stomatal closure in relation to the hydraulic vulnerability of the species (Martínez-Vilalta et al., 2014). We analysed the increase in PLC caused by the drought treatments applied (Δ PLC, with respect to the average PLC measured in *Ctrl* plants) with respect to g_L. This analysis clarifies that, during the applied drought, *O. carpinifolia* showed a more efficient stomatal control of embolism formation than *F. ornus* (see Supplementary Fig. S3).

In L_{dr+sh} plants, together with larger Ψ_{leaf_md} drops, *F. ornus* had lower Ψ_{tlp} than *O. carpinifolia*; this is consistent with previous studies (Bartlett et al., 2012; Bucci et al., 2004) and is explained by the fact that the maintenance of turgor at lower water potentials allows the preservation of water uptake and leaf hydraulic integrity during drought (Martorell et al., 2015). The Ψ_{tlp} adjustment during prolonged drought was accompanied by a decrease in π_0 (Table 1), which indicates the accumulation of solutes in the cells (Morgan, 1983) and is known to be a primary driver of Ψ_{tlp} decrease (Bartlett et al., 2012).

The response of NSC reserves to drought-induced variations in carbon supply is species-specific (Mitchell et al., 2014), and this explains the multidirectional patterns observed worldwide in NSC content at mortality (Adams et al., 2017). In our study species, wood NSC followed opposite patterns at the end of the long-term drought treatment accompanied by shading (L_{dr+sh} treatment), as well as at mortality (*Des* treatment). In *F. ornus* L_{dr+sh} plants, the decrease in NSC during drought, markedly driven by starch depletion, could have been caused by several processes. The maintenance of high carbon demands for growth and respiration, in parallel with a slow-down in photosynthesis, perhaps also associated with a decrease in sucrose transport from leaves (Sevanto, 2014), may have caused stem NSC depletion (McDowell et al., 2011; Mitchell et al., 2014). On the other hand, *O. carpinifolia* L_{dr+sh} plants maintained constant total NSC content, albeit this species was displaying a more isohydric strategy than *F. ornus*.

4.2. Hydraulic recovery in F. ornus is associated with high wood NSC content

Contrary to *O. carpinifolia, F. ornus* experienced high stem PLC (~80%) at the end of the drought period, in both L_{dr+sh} and S_{dr} plants (Fig. 4). Twenty-four hours after re-irrigation PLC of *F. ornus* returned to control levels in S_{dr}-*R* but not in L_{dr+sh}-*R* plants, despite the fact that Ψ_{leaf_em} was similar in the two groups. These contrasting patterns of hydraulic recovery are in agreement with the tendentially lower wood NSC concentration recorded in L_{dr+sh} plants at the end of the long drought and shade treatment, compared to S_{dr} plants, in which high PLC was caused by a short drought pulse that did not markedly affect NSC reserves. In *F. ornus*, *Ctrl* plants showed an intrinsically high variability in starch content, which caused the high variability in total NSC content (see above). This reflects and justifies an even higher variability seen among S_{dr} plants, because they were subjected to a short-term and abrupt drought. Therefore, albeit in *F. ornus* the difference in NSC content between S_{dr} and L_{dr+sh} plants is not statistically significant, it is remarkable that L_{dr+sh} plants did show strong and significant NSC depletion during drought compared to *Ctrl* plants, and did not recover PLC.

Starch stored in xylem parenchyma is suggested to be the source of soluble sugars involved in the active refilling of xylem conduits (Salleo et al., 2009) and a low starch content in the xylem sapwood may result in a delay or absence of this process (Nardini et al., 2018; Salleo et al., 2009; Savi et al., 2016). The fact that *F. ornus* exhibited fast hydraulic recovery only in plants which did not deplete sapwood NSC and in particular starch reserves, supports those hypotheses and findings. In *F. ornus*, while Ψ_{leaf_em} did not differ between the two re-irrigated groups and was relatively low (~ -0.9 MPa), the following midday Ψ_{stem_md} was less negative than Ψ_{leaf_em} only in S_{dr}-*R* plants ($\Psi_{stem\_md} = -0.3$ MPa; Fig. 3) while stomata were still relatively close (g_L similar to end stress values in both S_{dr}-*R* and L_{dr+sh}-*R* plants, Fig. 2). This probably indicates that the restoration of xylem hydraulics also favoured the recovery of water potential.

Stem NSC content has been positively related to wood parenchyma fraction (Plavcová et al., 2016) and to the recovery capability of tree species (Savi et al., 2016). Consequently, it can be hypothesized that *O. carpinifolia*, which had intrinsically lower stem NSCs contents, might possess a lower hydraulic recovery capability than *F. ornus*. Unfortunately, we could not test the short-term refilling capability of *O. carpinifolia*, given that L_{dr+sh} and S_{dr} plants did not suffer embolism at the peak of drought. Further experiments in plants subjected to more negative Ψ_{stem_md} before re-irrigation should shed light into the possible recovery potential of this as well as other relatively isohydric species.

4.3. Causes of mortality

In the present study, hydraulic failure occurred in both species at mortality (PLC > 90%), but NSC depletion was only observed in *F. ornus*, given that *Des* plants of *O. carpinifolia* had NSC contents similar to *Ctrl* plants. In *F. ornus*, instead, we observed both PLCs above 90% and a consistent and significant depletion in total NSCs in both wood and bark tissue at mortality. A severe drought spell that occurred in 2012 in a Karstic area induced in *F. ornus* adult trees extensive crown desiccation, which was likely related to hydraulic failure (Nardini et al., 2013). In the light of our results and given that no information on NSC content was available in that study, it would be of great interest to include NSC analyses in future field studies on mortality of this species. In *O. carpinifolia* adult trees from the same Karstic area, PLC reached 60% at the peak of drought in summer, that was related to Ψ_{stem_md} of ~ -3.0 MPa (Nardini et al., 2016) and visible crown die-back. However, just like in our saplings brought to death and hydraulic failure (*Des* plants), NSCs were not depleted in adult plants and instead an increase in soluble NSCs was detected at the peak of drought (Nardini et al., 2016).

Our data confirm that carbon starvation simply defined as a reduction of NSC pools is not ubiquitous at tree mortality (Adams et al., 2017) and may not occur in *O. carpinifolia*. Probably, carbon starvation is favoured by a wide carbon safety margin (see Mitchell et al., 2014) coupled with prolonged and sufficient hydration (i.e. a slow desiccation process) that allows the depletion of NSC reserves before marked tissue dehydration.

5. Conclusions

Our study sheds light into the importance of drought intensity and duration on hydraulic damage and recovery in two co-occurring woody species with contrasting water use strategies. Most importantly, our data demonstrate that adequate NSC availability in the wood at the end of drought could be a crucial factor determining the capacity of a species to recover hydraulic function. In particular, given the functional role of NSCs stored in the living cells of the stem wood fraction and that NSC dynamics can be different between wood and bark, we recommend to analyse separately the NSC content in the two tissues. In the past few years, a growing number of studies has underlined the involvement of NSCs not only in the maintenance of water transport during drought (e.g. Bloemen et al., 2016; O'Brien et al., 2014; Sevanto et al., 2014) but also in the hydraulic recovery upon irrigation (e.g. Savi et al., 2016; Tomasella et al., 2017; Trifilò et al., 2017; Yoshimura et al., 2016; Zeppel et al., 2019) or after frost events (Beikircher et al., 2016; Mayr et al., 2014). According to those studies and to ours here presented, we recommend to include the analysis of stem NSC content in future studies evaluating the recovery of hydraulic function of trees.

Contributions

A.N., V.C., T.S. and P.T. designed the experiment; N.A, T.S. and F.P. conducted the experiment; M.T., V.C. and N.A. conducted NSC analyses; F.P. and M.T. conducted statistical analyses and prepared the figures; M.T. wrote the manuscript; all authors commented and contributed to the final version of the manuscript.

Acknowledgements

The study was funded by the Fondazione Beneficentia Stiftung (Project title: Cambiamenti climatici e mortalità degli alberi: basi genotipiche della resistenza e resilienza a eventi estremi di aridità). N.A. was supported by the "Grant for Short-Term Mobility (KUWI) Theses and Specialized Courses Abroad" of the University of Graz. We thank the "Direzione centrale risorse agroalimentari, forestali e ittiche – area foreste e territorio" of the "Regione autonoma Friuli Venezia Giulia" and the public nursery Vivai Pascul (Tarcento, Italy) for providing the plant material for the experiment.

Appendix A. Supplementary data

Supplementary data to this article can be found online at https://doi.org/10.1016/j.plaphy.2019.10.024.

References

Adams, H.D., Zeppel, M.J.B., Anderegg, W.R.L., Hartmann, H., Landhausser, S.M., Tissue, D.T., Huxman, T.E., Hudson, P.J., Franz, T.E., Allen, C.D., et al., 2017. A multi-species synthesis of physiological mechanisms in drought-induced tree mortality. Nat. Ecol. Evol. 1, 1285–1291.

Bartlett, M.K., Scoffoni, C., Sack, L., 2012. The determinant of leaf turgor loss point and prediction of drought tolerance of species and biomes: a global meta-analysis. Ecol. Lett. 15, 393–405.

Beikircher, B., Mittmann, C., Mayr, S., 2016. Prolonged soil frost affects hydraulics and phenology of apple trees. Front. Plant Sci. 7, 867.

Bloemen, J., Vergeynst, L.L., Overlaet-Michiels, L., Steppe, K., 2016. How important is woody tissue photosynthesis in poplar during drought stress? Trees 30, 63–72.

Brodersen, C.R., McElrone, A.J., 2013. Maintenance of xylem network transport capacity: a review of embolism repair in vascular plants. Front. Plant Sci. 4, 108.

Brodribb, T.J., Bowman, D.J.M.S., Nichols, S., Delzon, S., Burlett, R., 2010. Xylem function and growth rate interact to determine recovery rates after exposure to extreme water deficit. New Phytol. 188, 533–542.

Bucci, S.J., Goldstein, G., Meinzer, F.C., Scholz, F.G., Franco, A.C., Bustamante, M., 2004. Functional convergence in hydraulic architecture and water relations of tropical savanna trees: from leaf to whole plant. Tree Physiol. 24, 891–899.

Caldeira, M.C., Lecomte, X., David, T.S., Pinto, J.G., Bugalho, M.N., Werner, C., 2015. Synergy of extreme drought and shrub invasion reduce ecosystem functioning and resilience in water-limited climates. Sci. Rep. 5, 15110.

Deslauriers, A., Beaulieu, M., Balducci, L., Giovannelli, A., Gagnon, M.J., Rossi, S., 2014. Impact of warming and drought on carbon balance related to wood formation in black spruce. Ann. Bot. 114, 335–345.

Fu, X., Meinzer, F.C., 2019. Metrics and proxies for stringency of regulation of plant water status (iso/anisohydry): a global data set reveals coordination and trade-offs among water transport traits. Tree Physiol. 39, 122–134.

Hao, G.Y., Wheeler, J.K., Holbrook, N.M., Goldstein, G., 2013. Investigating xylem embolism formation, refilling and water storage in tree trunks using frequency domain reflectometry. J. Exp. Bot. 64, 2321–2332.

Hartmann, H., Trumbore, S., 2016. Understanding the roles of non-structural carbohydrates in forest trees – from what we can measure to what we want to know. New Phytol. 211, 386–403.

Hartmann, H., Ziegler, W., Trumbore, S., 2013. Lethal drought leads to reduction in non-structural carbohydrates in Norway spruce tree roots but not in the canopy. Funct. Ecol. 27, 413–427.

Hoch, G., Richter, A., Koerner, C., 2003. Non-structural carbon compounds in temperate forest trees. Plant Cell Environ. 26, 1067–1081.

Hochberg, U., Rockwell, F.E., Holbrook, N.M., Cochard, H., 2018. Iso/anisohydry: a plant-environment interaction rather than a simple hydraulic trait. Trends Plant Sci. 23, 112–120.

Kannenberg, S.A., Novik, K.A., Philips, R.P., 2017. Coarse roots prevent declines in whole-tree non-structural carbohydrate pools during drought in an isohydric and an anisohydric species. Tree Physiol. 38, 582–590.

Klein, T., 2014. The variability of stomatal sensitivity to leaf water potential across tree species indicates a continuum between isohydric and anisohydric behaviours. Funct. Ecol. 28, 1313–1320.

Klein, T., Hoch, G., Yakir, D., Koerner, C., 2014. Drought stress, growth and non-structural carbohydrate dynamics of pine trees in a semi-arid forest. Tree Physiol. 34, 981–992.

Klein, T., Zeppel, M.J.B., Anderegg, W.R.L., Bloemen, J., De Kauwe, M.G., Hudson, P., Ruehr, N.K., Powell, T.L., von Arx, G., Nardini, A., 2018. Xylem embolism refilling and resilience against drought-induced mortality in woody plants: processes and trade-offs. Ecol. Res. 33, 839–855.

Li, X., Blackman, C.J., Peters, J.M.R., Choat, B., Rymer, P.D., Medlyn, B.E., Tissue, D.T., 2019. More than iso/anisohydry: hydroscapes integrate plant water use and drought tolerance traits in 10 eucalypt species from contrasting climates. Funct. Ecol. 33, 1035–1049.

Martínez-Vilalta, J., Garcia-Forner, N., 2017. Water potential regulation, stomatal behaviour and hydraulic transport under drought: deconstructing the iso/anisohydric concept. Plant Cell Environ. 40, 962–976.

Martínez-Vilalta, J., Poyatos, R., Aguadé, D., Retana, J., Mencuccini, M., 2014. A new look at water transport regulation in plants. New Phytol. 204, 105–115.

Martínez-Vilalta, J., Sala, A., Asensio, D., Galiano, L., Hoch, G., Palacio, S., Piper, F.I., Lloret, F., 2016. Dynamics on non-structural carbohydrates in terrestrial plants: a global synthesis. Ecol. Monogr. 86, 495–516.

Mayr, S., Schmid, P., Laur, J., Rosner, S., Charra-Vaskou, K., Daemon, B., Hacke, U.G., 2014. Uptake of water via branches helps timberline conifers refill embolized xylem in late winter. Plant Physiol. 164, 1731–1740.

Mooney, H., 1972. The carbon balance of plants. Annu. Rev. Ecol. Evol. Syst. 3, 315–346.

McDowell, N.G., Pockman, W.T., Allen, C.D., Breshears, D.D., Cobb, N., Kolb, T., Plaut, J., Sperry, J., West, A., Williams, D.G., et al., 2008. Mechanisms of plant survival and mortality during drought: why do some plants survive while others succumb to drought? New Phytol. 178, 719–739.

McDowell, N.G., Beerling, D.J., Breshears, D.D., Fisher, R.A., Raffa, K.F., Stitt, M., 2011. The interdependence of mechanisms underlying climate-driven vegetation mortality. Trends Ecol. Evol. 26, 523–532.

Meinzer, F.C., Woodruff, D.R., Marias, D.R., Smith, D.D., McCulloh, K.A., Howard, A.R., Magedman, A.L., 2016. Mapping 'hydroscapes' along the iso- to anisohydric continuum of stomatal regulation of plant water status. Ecol. Lett. 19, 1343–1352.

Mitchell, P.J., O'Grady, A.P., Tissue, D.T., White, D.A., Ottenschlaeger, M.L., Pinkard, E.A., 2013. Drought response strategies define the relative contributions of hydraulic dysfunction and carbohydrate depletion during tree mortality. New Phytol. 197, 862–872.

Mitchell, P.J., O'Grady, A.P., Tissue, D.T., Worledge, D., Pinkard, E.A., 2014. Co-ordination of growth, gas exchange and hydraulics define the carbon safety margins in tree species with contrasting drought strategies. Tree Physiol. 34, 443–458.

Morgan, J.M., 1983. Osmoregulation and water stress in higher plants. Annu. Rev. Plant Physiol. 35, 299–319.

Nardini, A., Salleo, S., Trifilò, P., Lo Gullo, M.A., 2003. Water relations and hydraulics characteristics of three woody species co-occurring in the same habitat. Ann. For. Sci. 60, 297–305.

Nardini, A., Gascò, A., Trifilò, P., Lo Gullo, M.A., Salleo, S., 2007. Ion-mediated enhancement of xylem hydraulic conductivity is not always suppressed by the presence of Ca^{2+} in the sap. J. Exp. Bot. 58, 2609–2615.

Nardini, A., Lo Gullo, M.A., Salleo, S., 2011. Refilling of embolized conduits: is it a matter of phloem unloading? Plant Sci. 180, 604–611.

Nardini, A., Battistuzzo, M., Savi, T., 2013. Shoot desiccation and hydraulic failure in temperate woody angiosperms during an extreme summer drought. New Phytol. 200, 322–329.

Nardini, A., Savi, T., Novak, M., 2014. Droughts, heat waves and plant hydraulics: impacts and legacies. Agrochimica 58, 146–161.

Nardini, A., Casolo, V., Dal Borgo, A., Savi, T., Stenni, B., Bertoncin, P., Zini, L., McDowell, N.G., 2016. Rooting depth, water relations and non-structural carbohydrate dynamics in three woody angiosperms differentially affected by an extreme summer drought. Plant Cell Environ. 39, 618–627.

Nardini, A., Savi, T., Losso, A., Petit, G., Pacilè, S., Tromba, G., Mayr, S., Trifilò, P., Lo Gullo, M.A., Salleo, S., 2017. X-ray micro-tomography observations of xylem embolism in stems of *Laurus nobilis* L. are consistent with hydraulic measurements of percent loss of conductance. New Phytol. 213, 1068–1075.

Nardini, A., Savi, T., Trifilò, P., Lo Gullo, M.A., 2018. Drought stress and the recovery from xylem embolism in woody plants. Prog. Bot. 79, 197–231.

O'Brien, M.J., Leuzinger, S., Philipson, C.D., Hector, T.J., 2014. Drought survival of tropical tree seedlings enhanced by non-structural carbohydrate levels. Nat. Clim. Chang. 4, 710–714.

Ogasa, M., Miki, N., Yoshikawa, K., 2010. Changes of hydraulic conductivity during dehydration and rehydration in *Quercus serrata* Thunb. and *Betula platyphylla* var. japonica Hara: the effect of xylem structures. Tree Physiol. 30, 608–617.

Petruzzellis, F., Nardini, A., Savi, T., Tonet, V., Castello, M., Bacaro, G., 2019. Less safety for more efficiency: water relations and hydraulics of the invasive tree *Ailanthus altissima* (Mill.) Swingle compared with the native *Fraxinus ornus* L. Tree Physiol. 39, 76–87.

Pinheiro, J., Bates, D., Debroy, S., Sarkar, D., R Core Team, 2016. Nlme nonlinear mixed effects models. R Package. Version 3.1-124.

Plavcová, L., Hoch, G., Morris, H., Ghiasi, S., Jansen, S., 2016. The amount of parenchyma and living fibers affects storage of nonstructural carbohydrates in young stems and roots of temperate trees. Am. J. Bot. 103, 603–612.

Salleo, S., Lo Gullo, M.A., Trifilò, P., Nardini, A., 2004. New evidence for a role of vessel-associated cells and phloem in the rapid xylem refilling of cavitated stems of *Laurus nobilis* L. Plant. Cell Environ. 27, 1065–1076.

Salleo, S., Trifilò, P., Esposito, S., Nardini, A., Lo Gullo, M.A., 2009. Starch-to-sugar conversion in wood parenchyma of field-growing Laurus nobilis plants: a component of the signal pathway for embolism repair. Funct. Plant Biol. 36, 815–825.

Savi, T., Andri, S., Nardini, A., 2013. Impact of different green roof layering on plant water status and drought survival. Ecol. Eng. 57, 188–196.

Savi, T., Casolo, V., Luglio, J., Bertuzzi, S., Trifilò, P., Lo Gullo, M.A., Nardini, A., 2016. Species-specific reversal of stem xylem embolism after a prolonged drought correlates to endpoint concentration of soluble sugars. Plant Physiol. Biochem. 106, 198–207.

Secchi, F., Zwieniecki, M.A., 2016. Accumulation of sugars in the xylem apoplast observed under water stress conditions is controlled by xylem pH. Plant Cell Environ. 39, 2350–2360.

Secchi, F., Pagliarani, C., Zwieniecki, M.A., 2017. The functional role of xylem parenchyma cells and aquaporins during recovery from severe water stress. Plant Cell Environ. 40, 858–871.

Sevanto, S., 2014. Phloem transport and drought. J. Exp. Bot. 65, 1751–1759.

Sevanto, S., McDowell, N.G., Dickman, I.T., Pangle, R., Pockman, W.T., 2014. How do trees die? A test of the hydraulic failure and carbon starvation hypotheses. Plant Cell Environ. 37, 153–161.

Tardieu, F., Simonneau, T., 1988. Variability among species of stomatal control under fluctuating soil water status and evaporative demand: modelling isohydric and anisohydric behaviours. J. Exp. Bot. 49, 419–432.

Tomasella, M., Häberle, K.-H., Nardini, A., Hesse, B., Machlet, A., Matyssek, R., 2017. Post-drought hydraulic recovery is accompanied by non-structural carbohydrate depletion in the stem wood of Norway spruce saplings. Sci. Rep. 7, 14308.

Tomasella, M., Nardini, A., Hesse, B.D., Machlet, A., Matyssek, R., Häberle, K.H., 2019. Close to the edge: effects of repeated severe drought on stem hydraulics and non-structural carbohydrates in European beech saplings. Tree Physiol. 39, 717–728.

Trifilò, P., Raimondo, F., Lo Gullo, M.A., Barbera, P.M., Salleo, S., Nardini, A., 2014. Relax and refill: xylem rehydration prior to hydraulic measurements favours embolism repair in stems and generates artificially low PLC values. Plant Cell Environ. 37, 2491–2499.

Trifilò, P., Casolo, V., Raimondo, F., Petrussa, E., Boscutti, F., Lo Gullo, M.A., Nardini, A., 2017. Effects of prolonged drought on stem non-structural carbohydrates content and post-drought hydraulic recovery in *Laurus noblis* L.: the possible link between carbon starvation and hydraulic failure. Plant Physiol. Biochem. 120, 232–241.

Trifilò, P., Kiorapostolou, N., Petruzzellis, F., Vitti, S., Petit, G., Lo Gullo, M.A., Nardini, A., Casolo, V., 2019. Hydraulic recovery from xylem embolism in excised branches of twelve woody species: relationships with parenchyma cells and non-structural carbohydrates. Plant Physiol. Biochem. 139, 513–520.

Trugman, A.T., Detto, M., Bartlett, M.K., Medvigy, D., Anderegg, W.R.L., Schwalm, C., Schaffer, B., Pacala, S.W., 2018. Tree carbon allocation explains forest drought-kill and recovery patterns. Ecol. Lett. 21, 1552–1560.

Tyree, M.T., Zimmermann, M.H., 2002. Xylem Structure and the Ascent of Sap, second ed. Springer Verlag, Germany.

Wiley, E., Hoch, G., Landhäusser, S.M., 2017. Dying piece by piece: carbohydrate dynamics in aspen (*Populus tremuloides*) seedlings under severe carbon stress. J. Exp. Bot. 68, 5221–5232.

Yoshimura, K., Saiki, S.T., Yazaki, K., Ogasa, M.Y., Shirai, M., Nakano, T., Yoshimura, J., Ishida, A., 2016. The dynamics of carbon stored in xylem sapwood to drought-induced hydraulic stress in mature trees. Sci. Rep. 6, 24513.

Yemm, E.W., Willis, A.J., 1954. The estimation of carbohydrates in plant extracts by Anthrone. Biochem. J. 54, 508–514.

Young, R., Gorelick, R., Xing, T., 2018. Seasonal bulk xylem pressure in temperate broadleaf eudicot trees: a case study for sugar long-distance transport and signalling. Tree Genet. Genomes 14, 56.

Zeppel, M.J.B., Anderegg, W.R.L., Adams, H.D., Hudson, P., Cook, A., Rumman, R., Eamus, D., Tissue, D.T., Pacala, S.W., 2019. Embolism recovery strategies and nocturnal water loss across species influenced by biogeographic origin. Ecol. Evol. 9, 5348–5361.